BNL-229146-2025-JAAM

High-performance n-Type Polymers Based on Multiple Electron-withdrawing Groups Decorated (E)-1,2-Di(thiophen-2-yl)ethene Building Blocks

J. Ma, R. Li

To be published in "Chemical Research in Chinese Universities"

November 2025

Photon Sciences

Brookhaven National Laboratory

U.S. Department of Energy

USDOE Office of Science (SC), Basic Energy Sciences (BES). Scientific User Facilities (SUF)

DISCLAIMER

High-Performance n-Type Polymers Based on Multiple Electron-Withdrawing Groups Decorated (*E*)-1,2-di(thiophen-2-yl)ethene Building Blocks

MA Jianeng[1], CHEN Yongsheng, [1] CHEN Jiawei, [1] TANG Jie,[2] LI Yanru[1], LI Ruiping,[3] YU Liyang,[2]✉ and FEI Zhuping[1]✉

The performance of n-type conjugated polymers lags far behind that of p-type polymers, which significantly restricts the development of organic electronics. The (*E*)-1,2-di(thiophen-2-yl)ethene (TVT) unit, owing to its unique advantages, has been widely applied in the design of p-type polymer semiconductors. Previous studies have demonstrated that introducing electron-withdrawing groups can lower the frontier orbital energy levels of polymers and enhance electron injection/transporting capabilities. Based on this, we proposed incorporating multiple electron-withdrawing groups, such as amide groups, fluorine atoms, and cyano groups, into the polymer backbones of TVT-based polymer to facilitate the electron transport. We successfully designed and synthesized the polymers TVTDA-4FTVT and TVTDA-2F2CNTVT. Both polymers exhibited low frontier orbital energy levels. Due to its mixed stacking mode, the organic field-effect transistor (OFET) device based on TVTDA-4FTVT demonstrated an electron mobility one order of magnitude higher than that of TVTDA-2F2CNTVT. TVTDA-4FTVT showed the highest electron mobility of 0.87 cm^2 V^{-1} s^{-1}, while TVTDA-2F2CNTVT exhibited the highest electron mobility of 0.049 cm^2 V^{-1} s^{-1}. Owing to its deeper lowest unoccupied molecular orbital (LUMO) level, the OFET devices based on TVTDA-2F2CNTVT showed good air stability after being placed in a natural environment for 15 days.

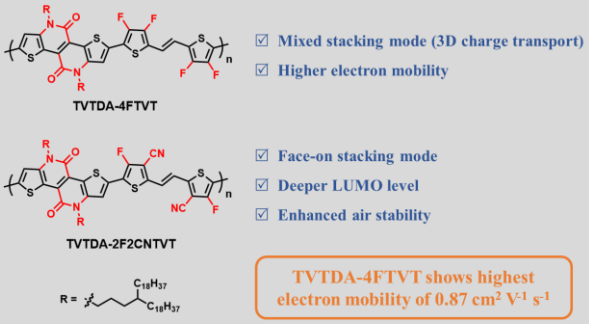

Keywords Organic field-effect transistor; electron-withdrawing groups; n-type; mobility; conjugated polymer

1 Introduction

In recent years, organic electronic devices have witnessed rapid development, with their performance being comparable to, or even surpassing, that of amorphous silicon devices in certain aspects.[1-4] As a typical representative of organic electronic devices, organic field-effect transistors (OFETs) exhibit broad potential application prospects in numerous fields, including radio frequency identification tags, sensors, flexible wearable devices, complementary logic circuits, and display drivers.[5-13] Organic semiconductors constitute a pivotal element within OFETs, with their carrier mobility serving as the crucial determinant of the devices' performance. Conjugated polymers, with their distinct advantages such as precise tunability of structure and function, solution-processability, light weight, low cost, and ease of large-scale device fabrication, have been widely applied in organic semiconductor layers.[14-19] Currently, p-type polymers have achieved relatively mature development, benefiting from a rich variety of molecular design strategies.[16, 20-25] The hole mobility of some D-A type polymers has even exceeded 10 cm^2 V^{-1} s^{-1}.[26, 27] However, the performance of n-type polymers lags significantly behind that of p-type polymers, manifesting as low electron mobility, high threshold voltage, and poor air stability.[13, 28-30] Given that n-type polymers play an indispensable role in complementary logic circuits, organic solar cells, and organic thermoelectrics,[28] there is an urgent need to address these issues to obtain n-type polymers with performance comparable to that of p-type polymers.

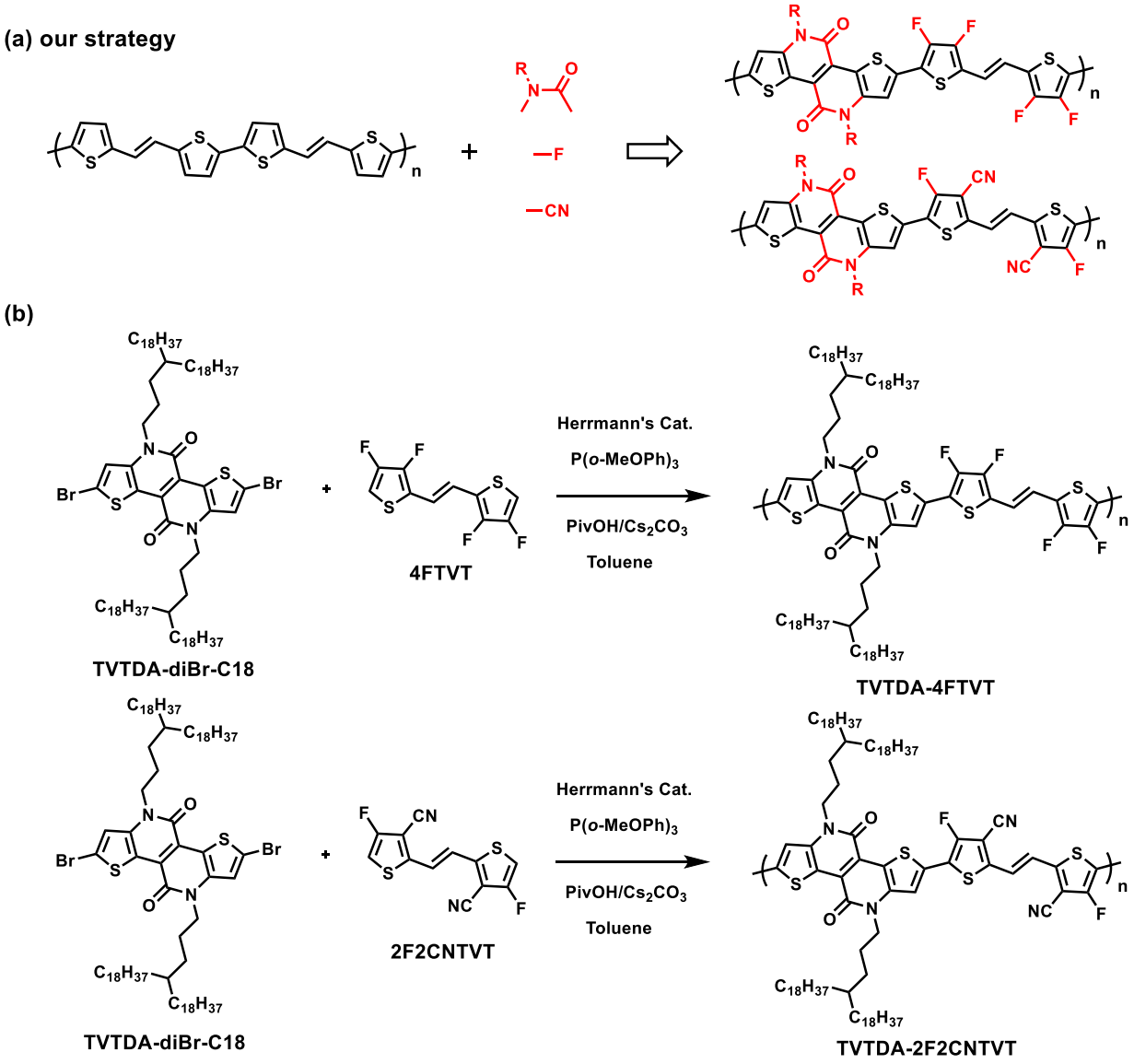

Scheme 1 (a) Our strategy to design n-type conjugated polymers, R=alkyl chains. (b) The synthetic route to polymers TVTDA-4FTVT and TVTDA-2F2CNTVT.

The root cause of these problems primarily lies in the insufficiently low frontier orbital energy levels of the polymers. To tackle this, electron-withdrawing groups can be introduced to simultaneously lower the highest occupied molecular orbital (HOMO) and lowest unoccupied molecular orbital (LUMO) energy levels of the polymers, thereby inhibiting hole injection while promoting electron injection and transport.[31] Amide and imide groups, as strong electron-withdrawing moieties, exhibit significant effects in regulating frontier orbital energy levels.[32] Additionally, side-chain modification on sp^3-hybridized nitrogen atoms can be employed to control molecular self-assembly behaviour and solution processability.[32, 33] Over the past few decades, researchers have designed numerous different building blocks containing amide and imide groups, such as PDI[34, 35], NDI[36-38], DPP[39-42], IID[43, 44], and BTI[45-47], for the development of high-performance polymers. The fluorine (F) atom also possesses strong electron affinity, enabling it to lower the frontier orbital energy levels of polymers without inducing steric hindrance.[48, 49] Furthermore, F atoms can induce the formation of intramolecular F···S and F···H interactions, enhancing the planarity of the main chain and shortening the intermolecular π-π stacking distance, thereby facilitating electron transport rates.[50-52] The cyano group exhibits even stronger electron-withdrawing ability than the F atom, allowing for a substantial reduction in energy levels.[29, 42] However, due to its relatively large size, careful consideration must be given to the selection of substitution positions.[30]

With its extended π-conjugation system and favourable planar structural characteristics, (E)-1,2-di(thiophen-2-

yl)ethene (TVT) has become a commonly used fundamental building block for designing high-performance conjugated polymers. However, most polymers prepared from TVT derivatives exhibit p-type or ambipolar performance characteristics, with only a very small number demonstrating n-type transport properties.[53-57] In our previous work, we developed the copolymers based on a TVT derivative, 2F2CNTVT, and the obtained polymers displayed purely n-type performance.[58] This further confirmed that introducing multiple electron-withdrawing groups onto the TVT unit is an effective strategy for constructing high-performance n-type polymers.

In this work, we introduced amide groups, fluorine atoms, and cyano groups onto TVT units, and successfully synthesized two n-type polymers, TVTDA-4FTVT and TVTDA-2F2CNTVT, by direct arylation polycondensation (DArP) (Scheme 1). Both polymers exhibited relatively low frontier orbital energy levels, which was beneficial for achieving efficient n-type charge injection/transport in OFETs. The device based on TVTDA-4FTVT exhibited optimal electron mobility performance at an annealing temperature of 250 °C, with a maximum electron mobility reaching 0.87 $cm^2 V^{-1} s^{-1}$, while the device based on TVTDA-2F2CNTVT achieved a maximum electron mobility of 0.049 $cm^2 V^{-1} s^{-1}$ at an annealing temperature of 200 °C. The electron mobility of TVTDA-4FTVT was an order of magnitude higher than that of TVTDA-2F2CNTVT, primarily due to the unique mixed stacking mode of TVTDA-4FTVT. Compared to TVTDA-4FTVT, the performance of the TVTDA-2F2CNTVT device showed no significant degradation after being placed under ambient conditions for 15 days, demonstrating superior air stability, which is mainly attributed to the deeper LUMO energy level of TVTDA-2F2CNTVT. This work provides significant guidance for the design of n-type polymers that combine high performance with high air stability.

2 Experimental

2.1 Chemicals and Materials

All chemicals and solvents were purchased from commercial sources without further purification unless otherwise indicated. Dichloromethane (DCM) was distilled from calcium hydride. Tetrahydrofuran (THF) and toluene were distilled from sodium and benzophenone ketyl under argon before use.

2.2 Experimental Instruments

NMR spectra were obtained in chloroform ($CDCl_3$) with TMS as the internal reference on a JNM-ECZ600R/S1 (JEOL, 600MHz) or JNM-ECZ400S/L (JEOL, 400MHz). The high-resolution mass spectrometry (HRMS) was performed on waters G2-XS Qtof (ionization mode: ESI). Absorption spectra were recorded on a UV-1900i (SHIMADZU) spectrophotometer. The electrochemical properties of these compounds were measured by Cyclic voltammetry on a CHI760E (SHANGHAICHENHUA). GPC analysis was recorded on a PL-GPC 220 system using 1,2,4-trichlorobenzene as the eluent and polystyrene as the standard at 150 °C. The thermogravimetric analysis (TGA) was conducted on a TG 209F3 thermogravimetric analyzer with a heating rate of 10 °C/min at a nitrogen flow. Differential scanning calorimetry (DSC) was carried out on a DSC214 polymer differential scanning calorimeter at a ±10 °C/min heating/cooling rate at a nitrogen flow. AFM measurements are carried out on a Dimension ICON (Bruker).

2.3 Synthetic Details

The synthetic routes to monomers and polymers, TVTDA-4FTVT and TVTDA-2F2CNTVT, are shown in Scheme S1 and Scheme 1(b), respectively. The synthesis details of intermediates are included in the Supporting Information. 4FTVT and 2F2CNTVT were synthesized according to literatures.[58, 59]

2.3.1 Synthesis of TVTDA-4FTVT

The reaction took place in a glovebox that was saturated with N_2: 4FTVT (25.7 mg, 0.097 mmol) and TVTDA-diBr-C18 (151.2 mg, 0.097 mmol), Herrmann's catalyst (1.8 mg, 0.0019 mmol), P(*o*-MeOPh)$_3$ (1.4 mg, 0.0040 mmol), pivalic acid (9.9 mg, 0.097 mmol), Cs_2CO_3 (95.1 mg, 0.29 mmol), and toluene (7 mL) were added to a 15 mL pressure-proof tube. After sealing with a cap in a glovebox, the mixture was stirred at 120 °C for 3 days. Then, the mixture was cooled to room temperature and was added dropwise to methanol. The crude polymer underwent filtration and was subsequently purified through a series of Soxhlet extractions using methanol, acetone, hexane, and chloroform as solvents. The chloroform solution was then concentrated, precipitated into methanol, filtered again, and finally dried under vacuum conditions to yield TVTDA-4FTVT (107 mg, yield: 66%). ^{1}H NMR (600 MHz, $CDCl_3$) δ(ppm): 7.43-6.46 (broad), 4.92-3.70 (broad), 2.03-1.15 (broad), 1.02-0.87 (broad). GPC: M_n = 32 kDa, M_w = 65 kDa,Đ = 2.05. $\lambda_{abs\ max}$ (film) = 684 nm.

2.3.2 Synthesis of TVTDA-2F2CNTVT

The reaction took place in a glovebox that was saturated with N_2: 2F2CNTVT (25.0 mg, 0.090 mmol) and TVTDA-diBr-C18 (139.8 mg, 0.090 mmol), Herrmann's catalyst (1.7 mg, 0.0018 mmol), P(*o*-MeOPh)$_3$ (1.3 mg, 0.0037 mmol), pivalic acid (9.2 mg, 0.090 mmol), Cs_2CO_3 (87.9 mg, 0.27 mmol), and toluene (7 mL) were added to a 15 mL pressure-proof tube. After sealing with a cap in a glovebox, the mixture was stirred at 120 °C for 3 days. Then, the mixture was cooled to room temperature and was added dropwise to methanol. The crude polymer underwent filtration and was subsequently purified through a series of Soxhlet extractions using methanol, acetone, hexane, and chloroform as solvents. The chloroform solution was then concentrated, precipitated into methanol, filtered again, and finally dried under vacuum conditions to yield TVTDA-2F2CNTVT. (128 mg, yield: 85%). ^{1}H NMR (600 MHz, $CDCl_3$) δ(ppm): 7.52-6.85 (broad), 4.95-3.77 (broad), 2.04-1.04 (broad), 1.02-0.82 (broad). GPC: M_n = 26 kDa, M_w = 67 kDa,Đ = 2.57. $\lambda_{abs\ max}$ (film) = 730 nm.

3 Results and Discussion

3.1 Synthesis

The detailed synthetic route for the dibromo monomer TVTDA-diBr-C18 required for the polymerization reaction is presented in detail in Scheme S1. Similar to our previous work,[60] high-purity *N*-alkylthiophen-3-amine (3) was synthesized through a two-step reaction. Subsequently, cyclization was achieved via an intermolecular aza-ene cycloaddition reaction, resulting in the formation of compound 4. In the subsequent reaction sequence, compound 4 underwent a series of reactions including hydrolysis, acyl chlorination, amidation, bromination, and a palladium-catalyzed C-H bond activation cyclization reaction, ultimately yielding TVTDA-C18.[61] The target dibromo monomer TVTDA-diBr-C18 was obtained by brominating TVTDA-C18 using *N*-bromosuccinimide (NBS) in yields of 69%. We utilized the highly reactive C-H bonds at the *α*-position of the thiophene rings in 4FTVT and 2F2CNTVT to carry out a green and efficient DArP with the dibromo monomer TVTDA-diBr-C18, successfully synthesizing the polymers TVTDA-4FTVT and TVTDA-2F2CNTVT in yields of 66% and 85%, respectively. It should be particularly noted that introducing fluorine atoms and cyano groups at the *β*-positions can effectively avoid coupling defects that may occur during the process, thereby preventing these defects from adversely affecting the polymer properties. The molecular weights of TVTDA-4FTVT and TVTDA-2F2CNTVT are 32 kDa and 26 kDa, respectively. The similar molecular weights allow for a fair comparison of the polymers' performance in subsequent studies.

3.2 Theoretical Calculations.

To further investigate the chain conformations and energy levels of these TVTDA-based polymers, density functional theory (DFT) calculations (Gaussian, B3LYP/6-31G**) were carried out. For the sake of streamlining the computational procedure, methyl groups were substituted in place of lengthy, branched alkyl side chains. The outcomes of these calculations are visually represented in Fig. 1 and Fig. S1. Since the distances between F···S, F···H, S···O, and S···H were all smaller than the sum of their respective van der Waals radii, multiple non-covalent interactions were present in both polymers. This resulted in a planar skeletal structure for each polymer, which was beneficial for charge transport. Compared to TVTDA-4FTVT, TVTDA-2F2CNTVT exhibited deeper HOMO and LUMO levels, along with a narrower bandgap, which can be attributed to the strong electron-withdrawing effect of the cyano group.

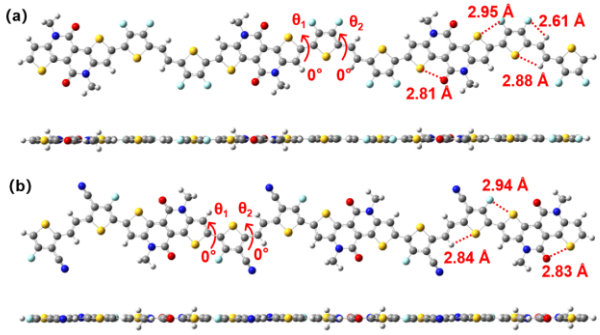

Fig.1 Top and side view of optimized conformation of (B3LYP-D3/6-31G(d,p)) methyl-substituted TVTDA-4FTVT (a) and TVTDA-2F2CNTVT (b).

3.3 Physicochemical properties.

To comprehensively characterize the photophysical properties of the polymers TVTDA-4FTVT and TVTDA-2F2CNTVT, we conducted UV-Vis-NIR spectroscopy absorption tests, and the absorption curves are shown in Fig. 2(a), and the data are summarized in Table 1. In the solution state, both polymers exhibit relatively broad absorption bands within the wavelength range of 400-800 nm. This absorption band can be attributed to the intramolecular charge transfer (ICT) effect. Specifically, the maximum absorption wavelengths of TVTDA-4FTVT and TVTDA-2F2CNTVT in chlorobenzene solution are 670 nm and 717 nm, respectively. Upon film formation, due to the more compact molecular packing, the maximum absorption peaks of both polymers exhibit a redshift phenomenon compared to those in the solution state. Compared to the TVTDA-4FTVT, the absorption peaks of TVTDA-

2F2CNTVT both in solution and film are located in the longer wavelengths, which can be attributed to the stronger electron-withdrawing ability of the cyano groups than that of the fluorine atoms, and hence enhancing the intramolecular charge transfer (ICT) effect. Consequently, the optical bandgap of TVTDA-2F2CNTVT is smaller than that of TVTDA-4FTVT, which is consistent with the DFT result. To evaluate the photophysical stability of the polymers, their dilute chlorobenzene solutions were exposed to natural light for 24 hours. A comparison of the UV-Vis-NIR absorption spectra before and after exposure (Fig. S2) reveals no notable alterations in either spectrum, indicating that both polymers exhibit good photophysical stability.

The thermal properties of the two polymers were characterized using thermogravimetric analysis (TGA) and differential scanning calorimetry (DSC), with the relevant results shown in Fig. S3 and S4, respectively. Both TVTDA-4FTVT and TVTDA-2F2CNTVT exhibit excellent thermal stability, with decomposition temperatures at 5% weight loss that are both higher than 440 °C. Within the temperature range of 50 °C - 200 °C, no obvious phase transition phenomena are observed in the DSC curves.

Table 1 Physical Properties of TVTDA-4FTVT and TVTDA-2F2CNTVT

Polymers	M_n (KDa)	Đ	T_d (°C)	$\lambda_{abs\ max}$ (sol) (nm)	$\lambda_{abs\ max}$ (film) (nm)	$E_{g,\ opt}$[a] (eV)	HOMO[b] (eV)	LUMO[c] (eV)
TVTDA-4FTVT	32	2.05	444	670	684	1.67	-5.60	-3.93
TVTDA-2F2CNTVT	26	2.57	443	717	730	1.54	-5.73	-4.19

[a]$E_{g,\ opt}$ = 1240/λ_{onset}; [b]HOMO were calculated from the Cyclic voltammogram (CV) data; [c]LUMO = HOMO – $E_{g,\ opt}$

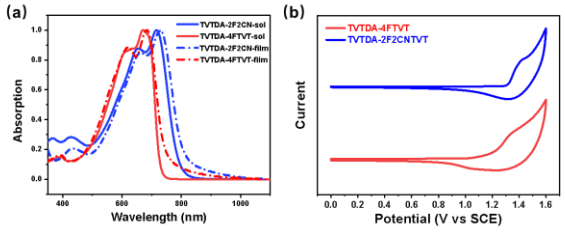

Fig.2 Normalized UV-Vis absorption spectra of the polymers in chlorobenzene solution and as a film state (a); Film cyclic voltammograms of the polymers with 0.1 M Bu_4NPF_6 in acetonitrile solutions under a scan rate of 50 mV/s (b).

To investigate the electrochemical properties of the polymers, cyclic voltammetry (CV) tests were conducted, with the relevant results shown in Fig. 2(b) and Table 1. Based on the oxidation potentials, the HOMO levels of the two polymers could be calculated. Specifically, the HOMO level of TVTDA-4FTVT was -5.60 eV, while that of TVTDA-2F2CNTVT was -5.73 eV. The LUMO levels of TVTDA-4FTVT and TVTDA-2F2CNTVT were calculated to be -3.93 and -4.19 eV, respectively. Both polymers possessed deep frontier orbital energy levels, which endowed them with the potential to become high-performance n-type polymers.

3.4 Organic Field-Effect Transistor Properties

We evaluated the charge transport characteristics of TVTDA-4FTVT and TVTDA-2F2CNTVT in top-gate/bottom-contact (TG/BC) field-effect transistors. On the Si/SiO_2 substrate, Au with a thickness of 32 nm was prepared as the source and drain electrodes through vacuum deposition and was modified with PEIE to effectively block hole injection. The polymer chlorobenzene solution with a concentration of 10 mg/mL was spin-coated to deposit the polymer thin film on the pre-patterned substrate, followed by annealing at different temperatures. After covering with a PMMA dielectric layer, Al was patterned using a mask of a specific size to serve as the gate electrode. The prepared OFET devices were tested under natural environmental conditions. Representative output characteristic curves and transfer characteristic curves are shown in Fig. 3, Fig. S5, and Fig. S6, respectively, and the relevant data are summarized in Table 2 and Table S1. The transfer curves of both polymers exhibit relatively small hysteresis. All the curves of $|I_D|^{1/2}$ versus V_G show a linear relationship without obvious inflection points, indicating that the devices have reliable mobilities.[62, 63] Due to their relatively low frontier orbital energy levels, all the OFET devices based on both polymers exhibit n-type transport characteristics. For devices based on TVTDA-4FTVT, when the annealing temperature was increased from 150 °C to 200 °C, their mobility significantly rose from 0.59 $cm^2\ V^{-1}\ s^{-1}$ to 0.85 $cm^2\ V^{-1}\ s^{-1}$ with I_{on}/I_{off} ratios of 10^3-10^4. A further increase in the annealing temperature to 250 °C had little impact on the mobility. For devices based on TVTDA-2F2CNTVT, when the annealing temperature was raised from 150 °C to 200 °C, the mobility improved from 0.032 $cm^2\ V^{-1}\ s^{-1}$ to 0.049 $cm^2\ V^{-1}\ s^{-1}$ with I_{on}/I_{off} ratios of 10^4-10^5. However, when the annealing temperature was further increased to 250 °C, the device performance notably declined, dropping to 0.029 $cm^2\ V^{-1}\ s^{-1}$. Compared to TVTDA-2F2CNTVT, the mobility of TVTDA-4FTVT was an order of magnitude higher.

The air stability of devices fabricated based on TVTDA-4FTVT and TVTDA-2F2CNTVT under ambient conditions (room temperature, relative humidity: 20%-40%) is presented in Fig. S9. After 15 days, the mobility of TVTDA-4FTVT was 0.72 $cm^2\ V^{-1}\ s^{-1}$, remaining at 86.7% of the

original value, which indicated its good air stability. For the device based on TVTDA-2F2CNTVT, its mobility remained almost unchanged with a value of 0.047 $cm^2 V^{-1} s^{-1}$ after being stored under the same conditions for 15 days. TVTDA-2F2CNTVT exhibited excellent stability, which was attributed to its deeper LUMO level that helped reduce electron traps induced by water and oxygen in the air.[64]

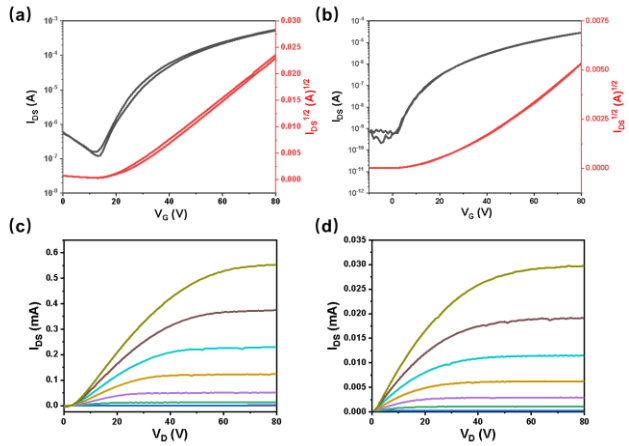

Fig.3 Typical transfer (a, b) and output characteristics (c, d) of TVTDA-4FTVT (a, c) and TVTDA-2F2CNTVT (b, d) based on TG/BC configuration OFETs devices annealed at 200 °C.

3.5 Thin Film Morphology and Microstructure

To delve deeply into the intrinsic relationship between the microstructure of polymer thin films and device performance, systematic characterization of the thin films was conducted using two-dimensional grazing-incidence wide-angle X-ray scattering (2D-GIWAX) and atomic force microscopy (AFM).

Table 2 OFET devices performance of TVTDA-4FTVT and TVTDA-2F2CNTVT in TG/BC device configuration annealed at 200 °C

Polymers	$\mu_{e,\ sat\ ave}$ ($\mu_{e,\ sat\ max}$) [$cm^2 V^{-1} s^{-1}$]	V_T (V)	I_{on}/I_{off}
TVTDA-4FTVT	0.83±0.01 (0.85)	-24±0.8	10^3-10^4
TVTDA-2F2CNTVT	0.048±0.001 (0.049)	-26±0.5	10^4-10^5

The GIWAX test results are presented in Fig. 4 and Fig. S10, respectively, with the one-dimensional fitting curves shown in Fig. S11 and the relevant data summarized in Tables S2 to S7. Comprehensive analysis reveals that, regardless of variations in the annealing temperature, TVTDA-4FTVT exhibited a prominent (010) diffraction peak in the out-of-plane (OOP) direction and multi-level lamellar stacking peaks (100), (200), and (300) in the in-plane (IP) direction, accompanied by characteristic π-π stacking peaks corresponding to (010). These diffraction features confirmed that TVTDA-4FTVT possessed a mixed stacking mode with coexisting edge-on and face-on orientations. In contrast, TVTDA-2F2CNTVT displayed weaker OOP (010) and IP (h00) peaks, predominantly demonstrating a face-on-dominated stacking mode. The mixed stacking mode significantly enhanced electron transport efficiency by constructing three-dimensional multi-channel pathways for carrier transport,[65-67] resulting in an electron mobility of TVTDA-4FTVT that was an order of magnitude higher than that of TVTDA-2F2CNTVT. For the TVTDA-2F2CNTVT system, at an annealing temperature of 150 °C, the π-π stacking distance in the IP direction was 4.05 Å, with a coherence length of 60.4 Å. As the annealing temperature increased to 200 °C and 250 °C, the π-π stacking distance remained unchanged, while the coherence length increased. This indicated a significant enhancement in the long-range order of π-π stacking along the gate-to-drain direction, thereby facilitating efficient electron transport along the source-to-drain electric field direction, which was consistent with the device testing results. For the TVTDA-2F2CNTVT system, when the annealing temperature was raised from 150 °C to 200 °C, the π-π stacking distance in the OOP direction shortened from 3.57 Å to 3.55 Å, and the coherence length increased from 31.6 Å to 31.9 Å; simultaneously, the lamellar stacking distance in the IP direction decreased from 17.30 Å to 17.11 Å, and the coherence length increased from 146.0 Å to 149.5 Å. These data changes indicated that annealing at 200 °C promoted tighter molecular arrangement, effectively facilitating electron interchain hopping transport and increasing the device mobility to 0.049 $cm^2 V^{-1} s^{-1}$. However, when the annealing temperature was further increased to 250 °C, although the π-π stacking distance continued to shorten to 3.53 Å, the lamellar stacking distances in both the OOP and IP directions exhibited an increasing trend. This might be attributed to the synergistic effect of the tighter arrangement of the main chains in the crystalline regions and a significant increase in the proportion of the amorphous regions, ultimately leading to a marked decline in the device performance of TVTDA-2F2CNTVT.

As depicted in the morphological images presented in Fig. 5 and Fig. S12, the fabricated polymer thin films uniformly displayed a continuous fibrous microstructure. When subjected to varying annealing temperatures, both the TVTDA-4FTVT and TVTDA-2F2CNTVT films demonstrated comparatively low surface roughness, a characteristic that is beneficial for facilitating electron transport.

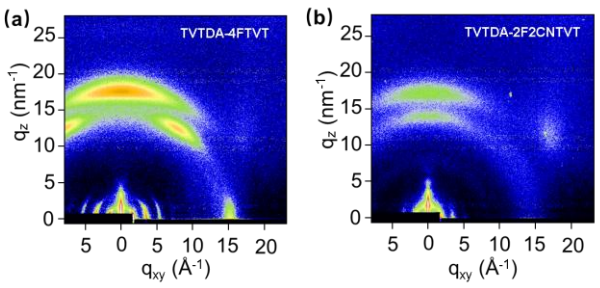

Fig.4 Two-dimensional GIWAXS images of TVTDA-4FTVT (a) and TVTDA-2F2CNTVT (b) films annealed at 200 °C.

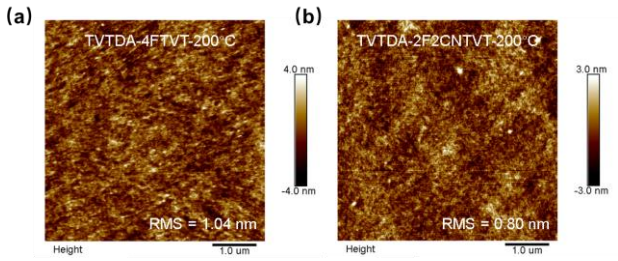

Fig.5 AFM topography images (5 μm × 5 μm) of spin-coated films of TVTDA-4FTVT (a) and TVTDA-2F2CNTVT (b) from CB solution (10 mg/mL) and subsequently annealed at 200 °C.

4 Conclusions

In this study, we designed and successfully synthesized two polymers, TVTDA-4FTVT and TVTDA-2F2CNTVT, by incorporating multiple electron-withdrawing groups into the TVT molecular backbone and utilizing the efficient DArP. Both polymers exhibited high molecular weights, planar backbone structure, deep frontier orbital energy levels, excellent thermal stability, and good photophysical stability. Notably, thanks to the more pronounced ICT effect induced by the cyano group, the absorption band of TVTDA-2F2CNTVT showed a significant red shift compared to that of TVTDA-4FTVT. The OFET device based on TVTDA-2F2CNTVT demonstrated the highest electron mobility of 0.049 $cm^2 V^{-1} s^{-1}$ at an annealing temperature of 200 °C, while the OFET device based on TVTDA-4FTVT achieved the highest electron mobility of 0.87 $cm^2 V^{-1} s^{-1}$ at an annealing temperature of 250 °C. The electron mobility of the TVTDA-4FTVT series devices was an order of magnitude higher than that of the TVTDA-2F2CNTVT series devices. This significant difference stemmed from the unique mixed stacking mode of TVTDA-4FTVT. Due to the deeper LUMO level of TVTDA-2F2CNTVT, the device based on TVTDA-2F2CNTVT exhibited no significant performance degradation after being placed in the environment for 15 days, demonstrating superior air stability. Our research provides guidance for the design of n-type polymers that exhibit both high performance and excellent air stability.

Electronic Supplementary Information

Supplementary material is available in the online version of this article at http://dx.doi.org/10.1007/s40242-023-3XXX-?.

Acknowledgements

The authors are grateful to the National Natural Science Foundation of China (21975176) and the Seed Foundation of Tianjin University (No. 2024XJD-0058). The authors also thank National Synchrotron Light Source II (NSLS-II, Contract No. DE- SC0012704) Brookhaven National Laboratory for providing GIWAXS experiment time.

Conflicts of Interest

The authors declare that they have no known competing financial interests or personal relationships that could have appeared to influence the work reported in this paper.

References

[1] Wang C., Zhang X. and Hu W., *Chemical Society Reviews*, **2020**, 49, *3*, 653-670.
[2] Paterson A. F., Singh S., Fallon K. J., Hodsden T., Han Y., Schroeder B. C., Bronstein H., Heeney M., McCulloch I. and Anthopoulos T. D., *Advanced Materials*, **2018**, 30, *36*, 1801079.
[3] Yang J., Zhao Z., Wang S., Guo Y. and Liu Y., *Chem*, **2018**, 4, *12*, 2748-2785.
[4] Sirringhaus H., *Advanced Materials*, **2014**, 26, *9*, 1319-1335.
[5] Kwon H.-j., Tang X., Shin S., Hong J., Jeong W., Jo Y., An T. K., Lee J. and Kim S. H., *ACS Applied Materials & Interfaces*, **2020**, 12, *27*, 30600-30615.
[6] Tang X., Murali G., Lee H., Park S., Lee S., Oh S. M., Lee J., Ko T. Y., Koo C. M., Jeong Y. J., An T. K., In I. and Kim S. H., *Advanced Functional Materials*, **2021**, 31, *29*, 2010897.
[7] Fukuda K., Takeda Y., Yoshimura Y., Shiwaku R., Tran L. T., Sekine T., Mizukami M., Kumaki D. and Tokito S., *Nature Communications*, **2014**, 5, *1*, 4147.
[8] Baeg K.-J., Caironi M. and Noh Y.-Y., *Advanced Materials*, **2013**, 25, *31*, 4210-4244.
[9] Yao Y., Dong H. and Hu W., *Advanced Materials*, **2016**, 28, *22*, 4513-4523.
[10] Klauk H., *Chemical Society Reviews*, **2010**, 39, *7*, 2643-2666.
[11] Zhu X., Zhang S.-R., Zhou Y. and Han S.-T., *Polymer International*, **2021**, 70, *4*, 358-366.
[12] Xie Y., Ding C., Jin Q., Zheng L., Xu Y., Xiao H., Cheng M., Zhang Y., Yang G., Li M., Li L. and Liu M., *SmartMat*, **2024**, 5, *4*, e1261.
[13] Quinn J. T. E., Zhu J., Li X., Wang J. and Li Y., *Journal of Materials Chemistry C*, **2017**, 5, *34*, 8654-8681.
[14] Yan L., Su N., Yang Y., Li X., Sun J., Wang S., Zhao L., Ding L. and Ding J., *SmartMat*, **2024**, 5, *5*, e1272.
[15] Liu J., Li W., Xian K., Liu Z., Li Y., Yao X., Ye L., Zhao Y. and Fei Z., *Chinese Journal of Chemistry*, **2023**, 41, *19*, 2525-2530.
[16] Wei X., Zhang W. and Yu G., *Advanced Functional Materials*, **2021**, 31, *21*, 2010979.
[17] Shi L., Guo Y., Hu W. and Liu Y., *Materials Chemistry Frontiers*, **2017**, 1, *12*, 2423-2456.
[18] Luo N., Ren P., Feng Y., Shao X., Zhang H.-L. and Liu Z., *The Journal of Physical Chemistry Letters*, **2022**, 13, *4*, 1131-1146.
[19] Xu J., Wang S., Wang G.-J. N., Zhu C., Luo S., Jin L., Gu X., Chen S., Feig V. R., To J. W. F., Rondeau-Gagné S., Park J., Schroeder B. C., Lu C., Oh J. Y., Wang Y., Kim Y.-H., Yan H., Sinclair R., Zhou D., Xue G., Murmann B., Linder C., Cai W., Tok J. B. H., Chung J. W. and Bao Z., *Science*, **2017**, 355, *6320*, 59-64.
[20] Zhang S., Liu Y., Dong H., Li Y., Zhang K., Xian K., Han Y., Ye L., Heeney M. and Fei Z., *Angewandte Chemie International Edition*, **2025**, 64, *19*, e202500860.
[21] Yang K., Chen Z., Wang Y. and Guo X., *Accounts of Materials Research*, **2023**, 4, *3*, 237-250.
[22] Kim M., Ryu S. U., Park S. A., Choi K., Kim T., Chung D. and Park T., *Advanced Functional Materials*, **2020**, 30, *20*, 1904545.
[23] Cheon H. J., An T. K. and Kim Y.-H., *Macromolecular Research*, **2022**, 30, *2*, 71-84.
[24] Liu Q., Bottle S. E. and Sonar P., *Advanced Materials*, **2020**, 32, *4*, 1903882.
[25] Hwang J., Shin J. and Lee W. H., *Macromolecular Research*, **2025**, 33, *1*, 1-14.
[26] Kang I., Yun H.-J., Chung D. S., Kwon S.-K. and Kim Y.-H., *Journal of the American Chemical Society*, **2013**, 135, *40*, 14896-

14899.
[27] Kim G., Kang S.-J., Dutta G. K., Han Y.-K., Shin T. J., Noh Y.-Y. and Yang C., *Journal of the American Chemical Society*, **2014**, 136, *26*, 9477-9483.
[28] Sun H., Guo X. and Facchetti A., *Chem*, **2020**, 6, *6*, 1310-1326.
[29] Kim H. S., Huseynova G., Noh Y.-Y. and Hwang D.-H., *Macromolecules*, **2017**, 50, *19*, 7550-7558.
[30] Chen J., Yang J., Guo Y. and Liu Y., *Advanced Materials*, **2022**, 34, *22*, 2104325.
[31] Zhao Y., Guo Y. and Liu Y., *Advanced Materials*, **2013**, 25, *38*, 5372-5391.
[32] Guo X., Facchetti A. and Marks T. J., *Chemical Reviews*, **2014**, 114, *18*, 8943-9021.
[33] Yang Y., Liu Z., Zhang G., Zhang X. and Zhang D., *Advanced Materials*, **2019**, 31, *46*, 1903104.
[34] Chen Z., Zheng Y., Yan H. and Facchetti A., *Journal of the American Chemical Society*, **2009**, 131, *1*, 8-9.
[35] Zhan X., Tan Z. a., Domercq B., An Z., Zhang X., Barlow S., Li Y., Zhu D., Kippelen B. and Marder S. R., *Journal of the American Chemical Society*, **2007**, 129, *23*, 7246-7247.
[36] Yan H., Chen Z., Zheng Y., Newman C., Quinn J. R., Dötz F., Kastler M. and Facchetti A., *Nature*, **2009**, 457, *7230*, 679-686.
[37] Zhao Z., Yin Z., Chen H., Zheng L., Zhu C., Zhang L., Tan S., Wang H., Guo Y., Tang Q. and Liu Y., *Advanced Materials*, **2017**, 29, *4*, 1602410.
[38] Al Kobaisi M., Bhosale S. V., Latham K., Raynor A. M. and Bhosale S. V., *Chemical Reviews*, **2016**, 116, *19*, 11685-11796.
[39] Nielsen C. B., Turbiez M. and McCulloch I., *Advanced Materials*, **2013**, 25, *13*, 1859-1880.
[40] Zhang X., Richter L. J., DeLongchamp D. M., Kline R. J., Hammond M. R., McCulloch I., Heeney M., Ashraf R. S., Smith J. N., Anthopoulos T. D., Schroeder B., Geerts Y. H., Fischer D. A. and Toney M. F., *Journal of the American Chemical Society*, **2011**, 133, *38*, 15073-15084.
[41] Yan X., Xiong M., Li J.-T., Zhang S., Chase Z. A., Lu Y., Wang Z.-Y., Yao Z.-F., Wang J.-Y., Gu X. and Lei T., *Journal of the American Chemical Society*, **2019**, 141, *51*, 20215-20221.
[42] Yun H.-J., Kang S.-J., Xu Y., Kim S. O., Kim Y.-H., Noh Y.-Y. and Kwon S.-K., *Advanced Materials*, **2014**, 26, *43*, 7300-7307.
[43] Gao Y., Deng Y., Tian H., Zhang J., Yan D., Geng Y. and Wang F., *Advanced Materials*, **2017**, 29, *13*, 1606217.
[44] Lei T., Cao Y., Fan Y., Liu C.-J., Yuan S.-C. and Pei J., *Journal of the American Chemical Society*, **2011**, 133, *16*, 6099-6101.
[45] Wei H., Liu Y., Liu Z., Guo J., Chen P.-A., Qiu X., Dai G., Li Y., Yuan J., Liao L. and Hu Y., *Advanced Electronic Materials*, **2020**, 6, *4*, 1901241.
[46] Guo X., Ortiz R. P., Zheng Y., Hu Y., Noh Y.-Y., Baeg K.-J., Facchetti A. and Marks T. J., *Journal of the American Chemical Society*, **2011**, 133, *5*, 1405-1418.
[47] Letizia J. A., Salata M. R., Tribout C. M., Facchetti A., Ratner M. A. and Marks T. J., *Journal of the American Chemical Society*, **2008**, 130, *30*, 9679-9694.
[48] Wang Y., Tan A. T.-R., Mori T. and Michinobu T., *Journal of Materials Chemistry C*, **2018**, 6, *14*, 3593-3603.
[49] Reichenbächer K., Süss H. I. and Hulliger J., *Chemical Society Reviews*, **2005**, 34, *1*, 22-30.
[50] Wang M., Ford M. J., Zhou C., Seifrid M., Nguyen T.-Q. and Bazan G. C., *Journal of the American Chemical Society*, **2017**, 139, *48*, 17624-17631.
[51] Huang H., Yang L., Facchetti A. and Marks T. J., *Chemical Reviews*, **2017**, 117, *15*, 10291-10318.
[52] Chen Z., Zhang W., Huang J., Gao D., Wei C., Lin Z., Wang L. and Yu G., *Macromolecules*, **2017**, 50, *16*, 6098-6107.
[53] Wei C., Tang Z., Zhang W., Huang J., Zhou Y., Wang L. and Yu G., *Polymer Chemistry*, **2020**, 11, *46*, 7340-7348.
[54] Sui Y., Shi Y., Deng Y., Li R., Bai J., Wang Z., Dang Y., Han Y., Kirby N., Ye L. and Geng Y., *Macromolecules*, **2020**, 53, *22*, 10147-10154.
[55] Guo K., Bai J., Jiang Y., Wang Z., Sui Y., Deng Y., Han Y., Tian H. and Geng Y., *Advanced Functional Materials*, **2018**, 28, *31*, 1801097.
[56] Chen H., Guo Y., Yu G., Zhao Y., Zhang J., Gao D., Liu H. and Liu Y., *Advanced Materials*, **2012**, 24, *34*, 4618-4622.
[57] Gao Y., Bai J., Sui Y., Han Y., Deng Y., Tian H., Geng Y. and Wang F., *Macromolecules*, **2018**, 51, *21*, 8752-8760.
[58] Zhang C., Tan W. L., Liu Z., He Q., Li Y., Ma J., Chesman A. S. R., Han Y., McNeill C. R., Heeney M. and Fei Z., *Macromolecules*, **2022**, 55, *11*, 4429-4440.
[59] Gao Y., Zhang X., Tian H., Zhang J., Yan D., Geng Y. and Wang F., *Advanced Materials*, **2015**, 27, *42*, 6753-6759.
[60] Su Y., Zhao L., Zhang S., Chen J., Li Y., Jiang T., Li J., Ji D., Li L. and Fei Z., *Chemical Research in Chinese Universities*, **2024**, 40, *6*, 1266-1274.
[61] Wang H.-C., Wang C.-C., Chen Y., Cao J., Ren X., Hong W. and Xu Y.-X., *Journal of Materials Chemistry C*, **2021**, 9, *38*, 13218-13225.
[62] McCulloch I., Salleo A. and Chabinyc M., *Science*, **2016**, 352, *6293*, 1521-1522.
[63] Bittle E. G., Basham J. I., Jackson T. N., Jurchescu O. D. and Gundlach D. J., *Nature Communications*, **2016**, 7, *1*, 10908.
[64] Nicolai H. T., Kuik M., Wetzelaer G. A. H., de Boer B., Campbell C., Risko C., Brédas J. L. and Blom P. W. M., *Nature Materials*, **2012**, 11, *10*, 882-887.
[65] Zhang C., Zheng Y., Li Y., Xue Z., Zhu X., Chen J., Ma J., Zhang Z., Zhong H., Yue W., Lei T. and Fei Z., *Advanced Functional Materials*, **2025**, 35, *23*, 2419706.
[66] Wang Y. and Takimiya K., *Advanced Materials*, **2020**, 32, *30*, 2002060.
[67] Ma M., Zhang L., Huang M., Kuang Y., Li H., Yang H., Yao T., Ye G., Shao S., Yoon M.-H. and Liu J., *Angewandte Chemie International Edition*, **2025**, 64, *21*, e202424820.